

Role of Core-Shell TiO₂-ZrO₂ Nanocomposite as a Visible Light Driven Catalyst

Priyanka Basyach¹, Madhabi Devi² and Amarjyoti Choudhury³

¹Digboi College

²Tezpur University

³USTM, Meghalaya

E mail: ¹pribasyach@gmail.com

Abstract—Here we report on a two step synthesis method of core shell TiO₂-ZrO₂ nanocomposites via a very cheap and simple sol-gel method. It is well known that TiO₂ exhibits very little absorbance in visible region. However its band gap may be altered by coating it with a shell layer. Such compounds show improved absorbance in visible regime than the core TiO₂. In our approach we used nanoscale ZrO₂ as the shell layer. The formation of core-shell nanostructure allows charge separation to occur at the interface due to difference in band alignment of the two materials. The synthesis of core-shell TiO₂-ZrO₂ nanocomposite was followed by studying optical properties through characterization tools such as UV and PL spectra. Also, we investigated the structural and morphological properties of the core-shell nanostructures with XRD patterns. The nanosize was confirmed via HRTEM images. A study on photocatalytic activity of the prepared core-shell nanocomposites under visible light is also performed for degradation of phenol which shows that the core-shell nanostructure induced way too better degradation than the core TiO₂ nanoparticle.

1. INTRODUCTION

Now a days, semiconductor nanostructures are regarded as established materials in the research field as they hold interesting optical and electrical properties leading to applications in photovoltaics and photocatalysis. Among them, core-shell nanocomposites have been able to grab quite an attention in the recent decades. Typically, a core-shell nanostructure is obtained by coating a lower energy gap nanomaterial by a higher energy gap material where the cores and shells may be any kind, i.e. metals, insulators and all classes of semiconductors[1]. The core-shell nanostructures are even divided into two distinct categories ; namely TYPE 1 and TYPE 2. Type 1 core-shell structures favour an enhanced luminescence due to higher degree of charge separation whilst the adverse effect is observed with TYPE 2 core-shell nanostructures whose band alignments lead to prominent charge separation.[2] Another type called inverted core-shell nanostructures are also reported where the core material is typically a higher band gap material and the shell material is a lower band gap material[3]. Again recent emergence due to environmental problems led the researchers to pay

considerable attention to the development of photocatalytic systems [4]. Various photocatalysts [4] are being studied with considerable interest due to photoelectrochemical solar-energy conversion. They could even be applied for the potential fields such as water splitting, self-cleaning surfaces, antimicrobialsystems, and the decomposition of organic pollutants [4]. Among the photocatalysts, TiO₂ has emerged as one of the most effective owing to its high photocatalytic efficiency, photostability, low cost, non-toxicity, and chemical inertness [4]. These advantages craft TiO₂ as a potential candidate for the photocatalytic decomposition of organic pollutants also [4]. But due to its high band gap, its photocatalytic activity is found to be limited to UV regime only . The recombination of photogenerated charge carriers (electron–hole pairs) also serve as another major drawback. To eliminate these constraints, band gap tuning of TiO₂ is performed by doping or coating with metal and nonmetal [4]. Several research groups have already been working extensively on decreasing the recombination rate of photogenerated electron–hole pairs using TiO₂ based heterogeneous catalysis materials. We have synthesized a core-shell nanostructure TiO₂-ZrO₂ where the shell is ZrO₂ with a band gap 5.7 eV and core TiO₂ has a band gap 3.25 eV. Although TiO₂-ZrO₂ has a TYPE 1 alignment in bulk form, coming down to nanosize it is found to exhibit properties of TYPE 2 core-shell structure. The optical and structural details are characterized via UV-vis absorbance spectra, PL spectra, XRD and TEM. The photocatalytic activity for both the samples are studied for degradation of Phenol under daylight illumination for different time limits.

2. MATERIALS AND METHODS

Titanium iso Propoxide, 2-Propanol, Zirconyl Nitrate Hydrate , Sodium Hydroxide and ethanol were used as the main reactant. For all washing and cleaning purpose , double distilled water was used. For the synthesis of core TiO₂ nanoparticles, we followed a standard procedure[5] where titanium isopropoxide, Ti{OCH(CH₃)₂}₄, was mixed with 2-propanol in a 2:5 ratio and stirred for 40 min for homogenous mixing. Then a few drops of water were added for hydrolysis

reaction to occur. For preparation of ZrO_2 coating layer, we followed an earlier report [6]. 2.312 g of $ZrO(NO_3)_2 \cdot xH_2O$ and 4 g of NaOH were dissolved, each in 20 ml of distilled water, to form 0.5 M and 5 M solutions, respectively. The NaOH solution was slowly added to the $ZrO(NO_3)_2 \cdot xH_2O$ solution under manual stirring. Then the resultant solution was poured dropwise on the already prepared TiO_2 nanoparticles under stirring which continued for 8 hours. Then the solution was centrifuged and dried at $100^\circ C$ to remove the water from the sample so that there can be a coating of ZrO_2 over the TiO_2 nanoparticles.

The UV-Visible DRS spectra of the samples were recorded in the range 300-700 nm using Shimadzu UV-2550 UV-Visible spectrophotometer. The photoluminescence spectra were recorded by a Persein-Eloven fluorescence spectrophotometer. Powder X-Ray diffraction (XRD) study was performed by a Rigaku Miniflex X-Ray diffractometer with $Cu K\alpha$ radiation ($\lambda = 1.5418 \text{ \AA}$) at 30 kV and 15 operating at with 2θ ranges from 10-70 degree. TEM characterization was done by a JEOL 2100 200 KV TEM instrument .

3. STRUCTURAL CHARACTERIZATIONS

3.1 XRD pattern

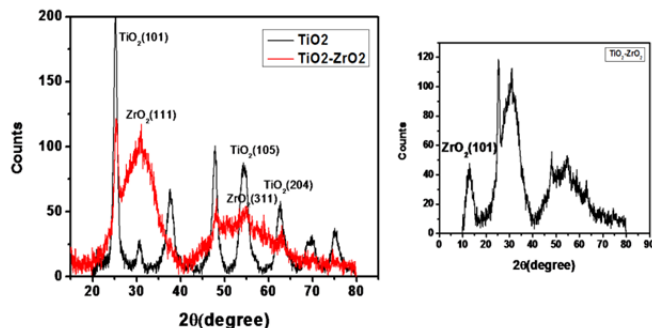


Fig. 1: (left) XRD pattern of TiO_2 nanoparticles and core-shell TiO_2/ZrO_2 nanostructures and (right) Extended version of XRD of TiO_2/ZrO_2 nanostructures

Fig. 1 shows the XRD pattern of core TiO_2 and core-shell TiO_2/ZrO_2 nanostructures. We can see that the core-shell nanostructure (red line) consists of both core TiO_2 and shell ZrO_2 phases. It contains anatase phase of core TiO_2 and monoclinic phase of shell ZrO_2 . The figure in the right hand side shows an extended version of the core-shell nanostructure where we can see the prime peak of ZrO_2 (101). The crystallite sizes were calculated using EVA diffraction software and the crystallite sizes are found to be around 8 nm for core TiO_2 nanostructures and 10 nm for core-shell TiO_2-ZrO_2 core-shell nanostructures. The crystallite sizes were estimated based on Bragg's law.

3.2 TEM image

The low resolution TEM image shows that the particles have sizes carrying from 5 nm- 20 nm. But the core-shell morphology is not clear in the low resolution image. From the

HRTEM image, the evidence of formation of core-shell is found as we can see two different types of lattice lanes which correspond to two different materials. The red colored planes are assigned to core TiO_2 and the yellow colored planes are drawn for the shell ZrO_2 .

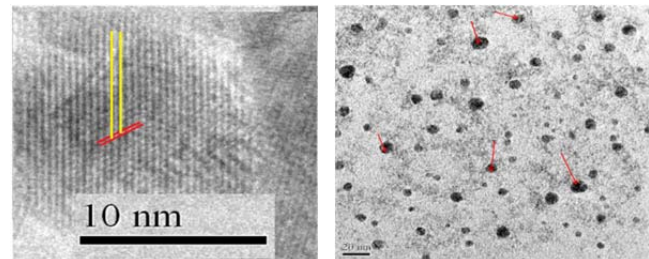


Fig. 2: (left) HRTEM image (right) Low resolution TEM image of core-shell TiO_2-ZrO_2 nanostructures

4. OPTICAL PROPERTIES

4.1 UV-Vis absorbance spectra

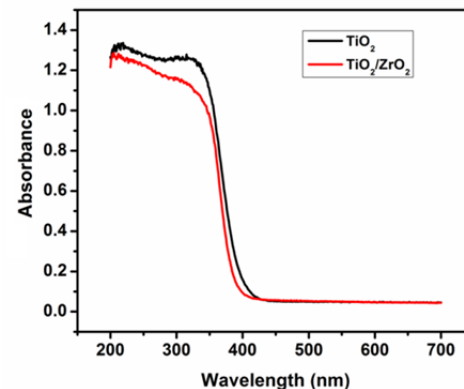
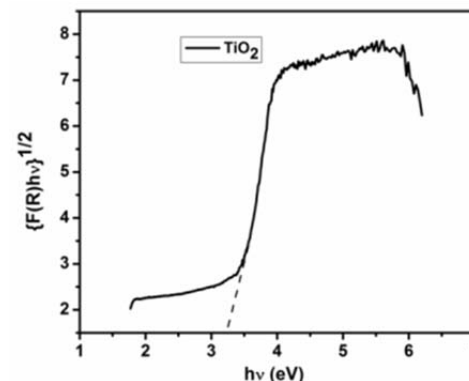


Fig. 3.1: UV-vis absorbance spectra

Fig. 3 shows the UV-vis absorbance spectra of core TiO_2 and core-shell TiO_2/ZrO_2 nanostructures. It is seen that absorbance maxima of TiO_2 which occurred at 350 nm is shifted to 355 nm after coating with ZrO_2 . This slight red shift occurs due to increase in particle size in the core-shell nanostructures. The absorption tail of TiO_2 in the visible region may be due to Ti^{3+} defect related states as well as oxygen vacancies present in the sample which goes for the core-shell structure.



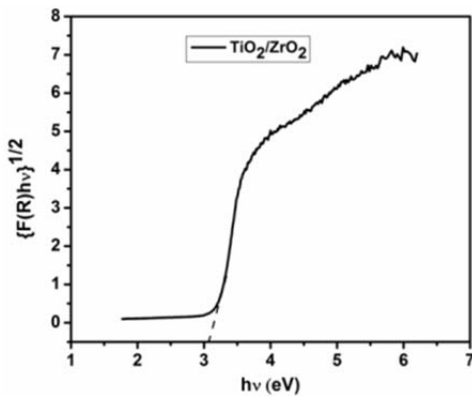


Fig. 3.2: Kubelka Munk Plot for (top) TiO₂ and (bottom) TiO₂-ZrO₂

The absorption is calculated by Kubelka-Munk plot $F(R) = (1 - R)^2 / 2R$, where R is the reflectance of the sample and it is found from the reflectance spectra. The band gap of the nanomaterials were calculated from a plot of the modified Kubelka-Munk function $[F(R) E]^{1/2}$ vs the energy of absorbed light $E (=h\nu)$ where $R=R_{\text{sample}}/R_{\text{BaSO}_4}$. After plotting the graphs and fitting linear, we get the band gap of TiO₂ to be 3.3 eV and TiO₂-ZrO₂ as 3.1 eV. The band gap of the core-shell structure is found to be lower than that of core one indicating the possibility of formation of a TYPE 2 structure which was later confirmed by PL spectra.

4.2 PL spectra

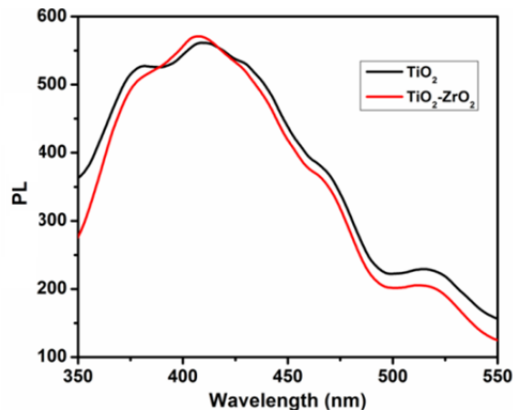


Fig. 4: PL spectra

Fig. 4 shows the comparative PL spectra of core TiO₂ and core-shell TiO₂-ZrO₂ nanostructures. It can be clearly seen from the figure that the intensity of the band edge emission peak is suppressed in the core-shell structure. If we look at the PL spectra, we can see that both core and the core-shell exhibit an emission peak at 380 nm. This peak is assigned to phonon assisted indirect transition from M→Γ in the Brillouin zone. The lowering of the peak is due to the coating layer of ZrO₂ surrounding TiO₂ as it does not allow sufficient amount of UV photons to go in and interact with the inner TiO₂ core

thus reducing the PL intensity. Both samples exhibit an intense emission peak around 425 nm which is attributed to self trapped exciton (STE) recombination [7-8]. The other peaks correspond to defect related states or oxygen vacancy related states. Thus the PL spectra also supports the quasi TYPE 2 structure in the core-shell structure which was earlier assumed from the band gap calculation.

5. PHOTOCATALYTIC ACTIVITY

Photocatalytic activities of pure TiO₂ nanoparticles and core-shell TiO₂-ZrO₂ nanoparticles are examined by observing the degradation of phenol under daylight. The photoactivity is observed under daylight lamp of 500 watt power Xenon lamp in the wavelength range from 400-700 nm. The samples are placed at 6 cm distance from the light in the photocatalysis chamber. The catalyst loaded dye solution is irradiated under daylight different time limits. When irradiation is completed, each of the irradiated solution is centrifuged at 13,000 rpm to make it free from the catalyst. 5 mL of each of the irradiated phenol solution is taken for absorption measurement. The decrease of concentration or degradation of phenol from its initial concentration is studied by observing the decrease of the absorption peak (A_t) of the dye solution irradiated for the aforementioned period. The degradation efficiency of phenol solution is given by $\{ (A_0 - A_t) / A_0 \} \times 100\%$ [9].

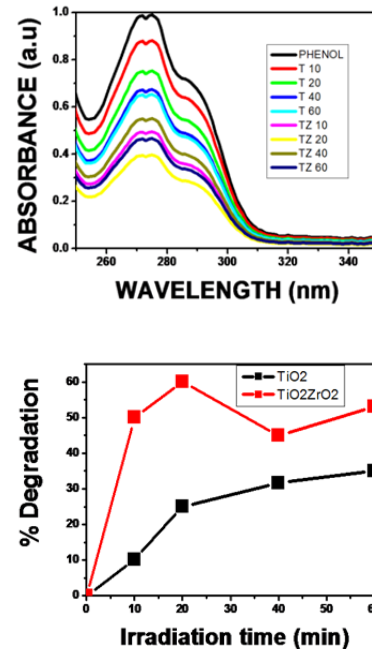


Fig. 5: (left) Absorbance of phenol in presence of catalyst (right) % degradation

Fig. 5 shows the degradation of phenol in presence of catalysts under visible light illumination.

Table 1: % Degradation of phenol under irradiation

Sample name	% degradation w.r.t time			
	10 min	20 min	40 min	60 min
TiO ₂	10.2	25	31.6	35
TiO ₂ /ZrO ₂	50	60	45	53

Table 1 clearly indicates that core-shell TiO₂-ZrO₂ nanostructures exhibit highest photocatalytic activity at 20 min irradiation which gradually increases from 10 min. Upon irradiation with light, lots of charge carriers (electron and holes) are created. However, light-generated electrons are found to be easily recombined in bulk or on the surface of the semiconductor. That is why, the photocatalytic efficiency of core TiO₂ is found to be so low. A light-generated hole may travel to the surface to take part in oxidation reactions with phenol and also to react with H₂O molecules present in the solution to form ·OH free radicals which further oxidize phenol [10]. But due to ambient charge separation present in TiO₂-ZrO₂ core-shell nanocomposites, the recombination rate of the charge carriers are lower than its core counterpart. Again the oxygen vacancy defect related states can easily capture the electrons and produce O²⁻ which is a strong oxidizing agent. It reacts directly with the phenol molecule causing its degradation.

6. CONCLUSION

Thus in this report, we have elaborated the optical as well as photocatalytic properties of core-shell nanocomposite TiO₂-ZrO₂. We have established from the spectroscopic analysis that the TYPE 1 core-shell s are transformed to TYPE 2 either due to generation of defect related states or size quantization effect. Also coating of ZrO₂ layer over TiO₂ greatly enhanced the photocatalytic activity by improving the charge separation at the interface of the core-shell nanostructure.

7. ACKNOWLEDGEMENT

Author 1 likes to acknowledge DST, Govt. of India for providing Inspire Fellowship during the research work while Author 3 acknowledges the financial support provided by Department of Science and Technology (DST), India, to the project SR/NM/NS-98/2010 (G) and also we want to thank SAIF, NEHU for helping us in carry-ing out the TEM measurement.

REFERENCE

- [1] Basyach.P and Choudhury,A.,” Structural and optical properties of core-shell Ag₂S/HgS nanostructures,” *Mat. Res. Bulletin*,48,2013pp. 2543-2548.
- [2] Ivanov.S.A, Piryatinski.A, Nanda.J Tretiak.S, Zavadii.K.R and Wal-lace.K.A et al .,” Type-II Core/Shell CdS/ZnSe Nanocrystals: Synthesis, Electronic Structures, and Spectroscopic Properties,”*J.Am.Chem.Soc.*, 129, 2007,pp. 11708-11719.
- [3] Balet.L.P, Ivanov.S.A, Piryatinski.A, Achermann.M and Klimov.V.I “In-verted Core/Shell Nanocrystals Continuously Tunable be-tween Type-I and Type-II Localization Regimes”,*Nano.Lett*,4,2004, pp. 1485 -1488.
- [4] Hwang.S.H, Kim.C and Jang J., ” SnO₂ nanoparticle embedded TiO₂ nanofibers — Highly efficient photocatalyst for the degradation of rhodamine B”, *Catalysis Communications*,12, 2011, pp. 1037–1041.
- [5] Mahshid.S,Ghamsari.M.S.Askari.M,Afshar.N and Lahuti.S.,”Synthesis TiO₂ nanoparticles by hydrolysis and peptization of titanium isopropoxide,”*SemiconductorPhysics,QuantumElectronics&Optoelectronics*,9,2006,pp.68.
- [6] Kumari.L, Li.W, and Wang.D., “Monoclinic zirconium oxide nanostructures synthesized by a hydrothermal route”, *nanotechnology*, 19, 2008, pp.195602-08.
- [7] Liu, J., et al. “Structure and photoluminescence study of TiO₂ nanoneedle texture along vertically aligned carbon nanofibre arrays”, *J. Phys. Chem. C.* 112, 2008, pp. 17127--17132.
- [8] Yu, J., et al. “Effects of F- doping on the photocatalytic and microstructure of nanocrystalline TiO₂ powders”, *Chem. Mater.* **14**, 2002, pp.3808-3816.
- [9] Choudhury, B., et al. “Extending Photocatalytic Activity of TiO₂Nanoparticles to Visible Region of Illumination by Doping of Cerium”, *Photochemistry and Photobiology*, 88, 2012, pp.257—264.
- [10] WANG.J.,et al. “Photocatalytic Degradation of Phenol-Containing Wastewater over Cu-Bi₂WO₆ Composite under Visible Light Irradiation”, *Journal of Residuals Science & Technology*, 9, 2012,pp.101-106.